Membrane Features and Activity of GPI-Anchored Enzymes: Alkaline Phosphatase Reconstituted in Model Membranes[†]

Silvia Sesana,[‡] Francesca Re,[‡] Alessandra Bulbarelli, Domenico Salerno, Emanuela Cazzaniga, and Massimo Masserini*

Department of Experimental Medicine, University of Milano-Bicocca, Monza, Italy

Received January 2, 2008; Revised Manuscript Received March 3, 2008

ABSTRACT: The influence of membrane lipid environment on the activity of GPI-anchored enzymes was investigated with human placental alkaline phosphatase reconstituted by a detergent-dialysis technique in liposomes composed of palmitoyloleoylphosphatidylcholine, alone or in mixture with lipids enriched along with the protein within lipid rafts: cholesterol, sphingomyelin, and GM1 ganglioside. The highest V_{max} was recorded for a phosphatidylcholine/10% GM1 mixture (143 ± 5 nmol of substrate hydrolyzed per minute per microgram of protein), while the lowest for a phosphatidylcholine/30% cholesterol mixture and for raft-mimicking 1:1:1 phosphatidylcholine/sphingolipid/cholesterol liposomes (M:M:M) (57 ± 3 and 52 ± 3, respectively). No significant differences in K_m were detected. The protein segregation, assessed using the chemical cross-linker bis(sulfosuccinimidyl)suberate, increased with the protein:lipid ratio, within the 1:1200−1:4800 protein:lipid molar ratio range, but did not affect enzyme activity. The activity decreased when the order of the lipid bilayers was increased, higher for those containing cholesterol, as judged by steady-state fluorescence polarization of 1,6-diphenyl-1,3,5-hexatriene. Finally, the GPI−enzyme activity was affected by membrane curvature. This result was suggested by a strong inverse correlation (Pearson's correlation coefficient = 0.91; $p < 0.0001$) between activity and liposome diameter, measured by laser light scattering and ranging between 59 ± 6 nm for a phosphatidylcholine/10% GM1 mixture (displaying the highest activity) and 188 ± 25 nm for a phosphatidylcholine/30% cholesterol mixture and 185 ± 23 nm for raft-mimicking liposomes (displaying the lowest activities). The activity−membrane curvature relationship was further confirmed by comparing the activity of proteoliposomes having different sizes but identical lipid compositions. These data open the possibility that the activity of GPI-anchored enzymes may be modulated by membrane microenvironment features, in particular by membrane curvature and cholesterol-enriched ordered microenvironments, such as those of lipid rafts.

Glycosylphosphatidylinositol (GPI)[1] anchor is a mode of membrane attachment for more than 200 eukaryotic cell-surface proteins (*1*). They are functionally diverse, ranging from adhesion molecules and surface antigens to receptors and hydrolytic enzymes (*2*), and are involved in different biological functions, especially in signal transduction and in the recognition process (*3*).

The detailed molecular structure of GPI anchors was determined for several proteins; they conserve a basic core covalently attached to the C-termini, consisting of a glycan moiety bound to phosphatidylinositol with two acyl chains embedded into the plasma membrane. Despite the extensive structural information available for the GPI moiety, the functional significance of this ubiquitous membrane anchorage, which is conserved from yeast to humans, is less understood. Especially in mammalian cells, the GPI moiety is thought to be more than just a membrane anchor and has been implicated in a variety of transmembrane and intracellular signaling, apical sorting, and cell−cell interaction events (*4–6*).

Several lines of evidence suggest that GPI-anchored proteins associate with putative cholesterol- and (glyco)sphingolipid-enriched platforms called "rafts" (*4–9*) and that such association is required for expression of their biological function (*8*). In the case of GPI-anchored enzymes, how the membrane microenvironment in which they are embedded may influence their activity is poorly understood. Therefore, we decided to approach this problem using, as the model system, liposomes embedding the GPI-anchored protein mammalian placental alkaline phosphatase (PLAP, EC 3.1.3.1).

MATERIALS AND METHODS

Chemicals. Palmitoyloleoylphosphatidylcholine (POPC), monosialoganglioside GM1 (GM1), and cholesterol (Chol) were from Avanti Polar Lipids (Alabaster, AL). Partially pure

[†] This investigation was supported by grants from MIUR, Italy (FIRB 2003, PRIN 2005 to M.M.).

* To whom correspondence should be addressed: Department of Experimental Medicine, University of Milano-Bicocca, Via Cadore 48, 20052 Monza (MI), Italy. Telephone: +39 0264488203. Fax: +39 0264488251. E-mail: massimo.masserini@unimib.it.

[‡] These authors contributed equally to this investigation.

[1] Abbreviations: GPI, glycosylphosphatidylinositol; BS^3, bis(sulfosuccinimidyl)suberate; PLAP, placental alkaline phosphatase; OctGlc, *n*-octyl β-D-glucoside; pNPP, *p*-nitrophenyl phosphate; PI-PLC, phosphatidylinositol-specific phospholipase C; POPC, 1-palmitoyloleoylglycero-3-phosphocholine; SM, sphingomyelin; GM1, monosialoganglioside GM1; Chol, cholesterol; DPH, 1,6-diphenyl-1,3,5-hexatriene; SCRL, sphingolipid−cholesterol-rich liposomes.

10.1021/bi800005s CCC: $40.75
Published on Web 04/17/2008

human placental tissue extract, *n*-octyl β-D-glucoside (OctGlc), *p*-nitrophenyl phosphate (pNPP), *p*-nitrophenol, sphingomyelin (SM), Triton X-114, phosphatidylinositol-specific phospholipase C (PI-PLC) from *Bacillus cereus*, bis(sulfosuccinimidyl)suberate (BS^3), Sephacryl 200 HR, bovine serum albumin, and the EZ-Blue staining kit were all from Sigma-Aldrich (Milano, Italy). 1,6-Diphenyl-1,3,5-hexatriene (DPH) was from Invitrogen (Carlsbad, CA). Reagents and gels for SDS−PAGE were purchased from Sigma-Aldrich and NuPAGE 1.5 mm, 4−12% gels from Invitrogen. All other chemicals were reagent grade.

Purification of Placental Alkaline Phosphatase (PLAP). PLAP was purified from a human placental tissue extract according to the method of Brown (*10*) with small modifications. For this purpose, 10 mg (as protein) of extract was dissolved in 2 mL of 1% (v/v) Triton X-114 in 10 mM Tris-HCl (pH 7.4) containing 150 mM NaCl, at 4 °C. The sample was vortexed and submitted to phase separation by incubation for 5 min at 30 °C, followed by centrifugation for 5 min at 300*g* at room temperature. After centrifugation, the lower phase (detergent-enriched phase) was recovered and supplemented with 1 mL of 10 mM Tris-HCl and 150 mM NaCl (pH 7.4). The phase separation step was repeated twice. The detergent phases were pooled and added with 20 mM OctGlc in phosphate-buffered saline (PBS) to obtain a final volume of 1.0 mL and then loaded on a Sephacryl 200 HR column (20 cm × 1.5 cm), pre-equilibrated and eluted with a PBS/OctGlc mixture. Protein elution was assessed by an enzymatic activity assay as described below. The protein purity of the fractions was assayed by SDS−PAGE according to the method of Laemmli (*11*), followed by Coomassie blue staining.

Enzyme Activity Assay and Kinetics. PLAP activity was assayed at 37 °C using 5 mM *p*-nitrophenyl phosphate (pNPP) as the substrate, in 25 mM glycine buffer (pH 10). The reaction was stopped by addition of 3 volumes of 1 M NaOH to the incubation mixture (*12*). The absorbance was measured spectrophotometrically at 420 nm. The amount of hydrolyzed substrate was assessed on the basis of a standard curve prepared with *p*-nitrophenol. PLAP kinetic parameters were determined by assaying the enzyme activity at substrate concentrations in the range of 0.05−5 mM. Michaelis−Menten constant (K_m) and the maximum velocity (V_{max}) values were determined from the double-reciprocal plot of 1/*V* versus 1/[S] according to the Lineweaver−Burk model (*13*) by linear regression and calculated with respect to the amount of outer-membrane-facing enzyme (see below).

Liposome and Proteoliposome Preparation. Liposomes and PLAP-embedding liposomes (proteoliposomes) were prepared by dialysis following the procedure described by Angrand et al. (*14*) with minor modifications. Liposomes were constituted by a matrix of POPC, alone or in binary, ternary, or quaternary mixtures with SM, GM1, or Chol, each present as a 10% molar proportion. Binary mixtures of POPC with SM and Chol were studied up to a molar proportion of 30%. Moreover, sphingolipid−cholesterol-rich liposomes (SCRL) composed of POPC, sphingolipids, and cholesterol (1:1:1, M:M:M) were utilized as a lipid raft-mimicking system, according to previous suggestions (*15, 16*).

Briefly, lipids (0.857 μmol) were mixed in the prefixed proportion in a 2:1 (v:v) chloroform/methanol mixture. Solvents were evaporated with a gentle stream of nitrogen followed by a vacuum pump for 3 h. The lipid film was then resuspended in 1.0 mL of a PBS/OctGlc mixture forming a lipid/detergent solution, then vortexed, and dialyzed (molecular mass cutoff of 12−14 kDa) for 24 h at a temperature above the T_m, determined by differential scanning calorimetry.

To obtain proteoliposomes, 20 μg of purified protein was added to the lipid/detergent solution and then dialyzed as described above. To study the influence of the protein:lipid molar ratio on enzyme activity, proteoliposomes were prepared at different protein:lipid molar ratios varying from 1:1000 to 1:5000 total lipids (corresponding to a protein:lipid ratio of ∼1:100 to 1:500 raft lipids) depending on the mixture. Unless otherwise specified, in most cases the protein was added to the lipid/detergent solution at a 1:3000 protein:lipid molar ratio.

In addition, to investigate the influence of bilayer curvature on enzyme activity, proteoliposomes of different diameters (100, 200, and 400 nm) composed of POPC were prepared. For this purpose, POPC multilamellar vesicles, prepared by resuspending a POPC lipid film in 1.0 mL of PBS obtained as described above, were extruded 10 times through polycarbonate filters (Millipore Corp., Bedford, MA) with pores 100, 200, and 400 nm in diameter using an extruder (Lipex Biomembranes, Vancouver, BC), as described previously (*17*). To obtain proteoliposomes, the technique described by Ronzon et al. (*18*) was utilized, consisting of the incubation of preformed liposomes with OctGlc, under conditions just destabilizing the lipid bilayer to promote protein insertion, followed by addition of enzyme and detergent removal.

The final lipid:protein molar ratio was assessed for each experiment as described below.

Purification and Characterization of Proteoliposomes. Proteoliposomes were separated from nonassociated PLAP by flotation on a discontinuous sucrose density gradient. For this purpose, samples (450 μL) of proteoliposomes, obtained as described above, were mixed with 1350 μL of 80% sucrose in PBS. Onto this suspension were layered 1350 μL of 50% sucrose in PBS and 1350 μL of PBS. The sample was centrifuged at 140000*g* for 2 h at 4 °C with a Beckman SW 40 TI rotor. Ten fractions of 450 μL each were collected from the top of the gradient and analyzed for lipid and protein content. The fractions containing both lipids and activity were taken to be the fractions containing proteoliposomes. Integration of PLAP in the membrane was assessed by spinning the proteoliposomes in a sucrose gradient (same as before) in the presence of 0.1 M Na_2CO_3 (pH 11) (*19*).

The protein and lipid recovery was assessed by a lipid and protein assay. For this purpose, phospholipids (POPC and SM) were determined by a phosphorus assay using the method of Bartlett (*20*). GM1 ganglioside content was determined as lipid-bound sialic acid by the method of Svennerholm (*21*), and cholesterol (Chol) content was determined as described previously (*22*). The protein concentration was measured using the bicinconic acid (BCA) kit, purchased from Bio-Rad (Hercules, CA); alternatively, the samples were resolved by SDS−PAGE followed by Comassie blue staining and densitometric analysis of PLAP bands. In both cases, known amounts of bovine serum albumin (BSA) were used as the standard. To determine the amount of residual Triton X-114 in the final proteoliposome preparations, total lipids were extracted from proteoliposomes according to the method of Giglioni et al. (*23*). The total

lipid extract was analyzed for the presence of Triton X-114 by measuring the OD at 275 nm and the detergent content calculated on the basis of the OD of Triton X-114 standard solutions.

To assess the distribution of PLAP in the two leaflets, proteoliposomes were incubated with PI-PLC for 2 h at 37 °C and a PLAP:PI-PLC activity ratio of 20 (U:U) and then spun on a discontinuous sucrose gradient to separate liposomes from detached PLAP (*14*). The anchorless PLAP was recovered at the bottom of the gradient and assayed by evaluation of enzyme activity and protein content. The liposome fraction, floating in the upper fractions of the gradient, was submitted to an activity assay before and after liposome disruption by treatment with 1% Triton X-100 (by volume).

Alternatively, the amount of outer-facing enzyme was measured on the basis of the accessibility to the substrate pNPP using intact proteoliposomes and then the total amount (outer- and inner-facing) of enzyme after liposome disruption by treatment with 1% Triton X-100 (by volume) (*14*). The proportion of outside-oriented enzyme was calculated as the ratio between the enzymatic activities measured before and after addition of Triton X-100.

Laser Light Scattering of Liposomes. The determination of the liposome size distribution was performed by the dynamic light scattering (DLS) method using a Brookhaven 90Plus system (Brookhaven Instruments Corp.). The technique measures Brownian motion of colloidal particles and relates this motion to their size. The liposomes are illuminated by a laser, and the light-scattered fluctuations arising from their Brownian motion are recorded. By studying the autocorrelation of the light intensity fluctuations, we obtain a mean size of liposomes. All the measurements were performed at room temperature by using a solid-state 652 nm laser, and the scattered light was detected at 90° with respect to the incidental beam.

Chemical Cross-Linking Analysis of PLAP. The protein cross-linking protocol described by Friedrichson (*24*) was utilized. Briefly, the cross-linking reaction was performed by incubation of proteoliposomes with 0.5 mM (final) BS^3 for 45 min at 4 °C. Unreacted cross-linker was quenched with 50 mM glycine for 15 min at 4 °C. Samples were resolved on a 4 to 12% SDS−PAGE gel followed by EZ-Blue staining, and bands were quantified by densitometric scanning (GS-710 calibrated imaging densitometer, Bio-Rad). The protein aggregation was expressed as the ratio between the OD of digitized bands corresponding to the cross-linked and non-cross-linked protein.

Diphenyl-1,3,5-hexatriene (DPH) Fluorescence Anisotropy Experiments. To measure DPH fluorescence polarization, 2 μL of a 10 mM solution of the probe in tetrahydrofuran were added under stirring to liposomes to obtain a final DPH:phosphorus molar ratio of 1:200. After incubation for 45 min at 37 °C in the dark under gentle stirring, DPH fluorescence was measured on a Cary Eclipse spectrofluorimeter (Varian) equipped with Glan-Thompson polarization filters. The fluorescence of samples without DPH was found to be negligible. Polarization values were always corrected for turbidity-dependent polarization, although, in most cases, these corrections amounted to less than 2% of the total polarization values.

Polarization (P) was calculated with the equation $P = (I_{VV} - I_{VH})/(I_{VV} + 2I_{VH})$, where I is emission intensity and the subscripts refer to the orientation (V for vertical and H for horizontal) of polarization filters in the excitation and emission beams, respectively. Polarization was measured successively at 37, 24, and 15 °C until shortly before the fluorescence was read in a sample chamber adjusted to the same temperature (*10*).

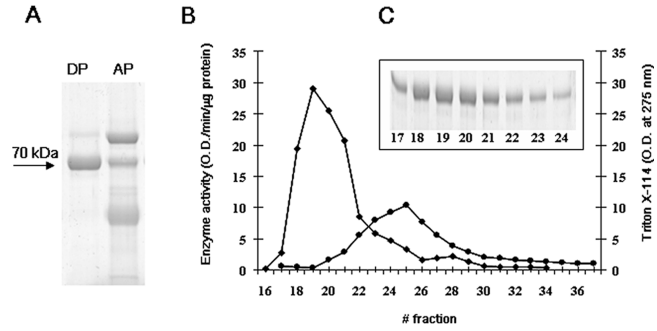

FIGURE 1: Illustration of the purification procedure of human placental alkaline phosphatase. (A) A commercial human placental extract was suspended in 1% Triton X-114, and after the mixture had been warmed at 30 °C, an aqueous phase (AP) and a detergent-enriched phase (DP) were obtained. Aliquots were submitted to SDS−PAGE followed by Coomassie blue staining. (B) The detergent-enriched phase was loaded on a Sephacryl 200 HR column and the enzyme elution followed by an enzymatic assay (◆) using *p*-nitrophenyl phosphate as a substrate, while the elution of Triton X-114 was followed by the OD at 275 nm (●). (C) Coomassie Blue staining of the SDS−PAGE gel carried out on fractions 17−24 eluted from the column.

Determination of the Protein Concentration. The protein concentration was measured with the bicinconic acid (BCA) kit, purchased from Bio-Rad (Hercules, CA), and by densitometric analysis of PLAP resolved by SDS−PAGE after Coomassie blue staining. In both cases, known amounts of BSA were used as the standard.

Statistical Analysis. The differences were evaluated for statistical significance using a Student's *t*-test, and a p value of <0.05 was considered to be significant. The relation among liposome diameter versus enzyme activity, DPH polarization versus enzyme activity, and DPH polarization versus liposome diameter was evaluated by assessing Pearson's correlation coefficient (r) and performing a linear regression test. GraphPad Prism 5 was used for statistical analysis.

RESULTS

Purification of PLAP. The commercial enzyme preparation was first submitted to phase separation using Triton X-114. The partitioning of proteins in the detergent-enriched phase with respect to proteins present in the aqueous phase is shown in Figure 1. The detergent phase was then submitted to gel filtration column chromatography to remove Triton X-114. The fractions displaying the presence of the enzyme, which eluted from the column before the elution of Triton X-114 (Figure 1), were pooled and used for the preparation of proteoliposomes. The purity of PLAP after the gel filtration step was >97%, as assessed by SDS−PAGE followed by Coomassie blue staining.

Preparation and Purification of Liposomes and Proteoliposomes. When PLAP was submitted to the dialysis procedure and ultracentrifugation in the absence of lipids, it was recovered at the bottom of the gradient. Lipids, submitted

to the dialysis procedure in the absence of PLAP, were recovered within the upper part of the gradient (usually fraction 3, data not shown). PLAP-embedding liposomes (proteoliposomes) were prepared by dialysis of dispersions of lipids and PLAP with OctGlu and submitted to purification by centrifugation in a discontinuous sucrose gradient. The fractions containing both lipids and protein were taken as the fractions containing purified proteoliposomes. Among these, the fraction having the highest activity (usually fraction 3, collected from the top of the gradient) was used. A demonstration that the protein was tightly integrated into the lipid bilayer was provided by control experiments, in which liposomes were prepared in the absence of the protein and then PLAP was added. After incubation at 37 °C for 10 min, the mixture was submitted to discontinuous sucrose gradient centrifugation: lipids were recovered in fraction 3 and PLAP was recovered at the bottom of the gradient (data not shown). A further demonstration that the protein was tightly integrated was shown by the resistance to treatment with Na_2CO_3 and subsequent flotation on a sucrose gradient (data not shown). The total lipid recovery ranged from 70 to 90% after dialysis; the lipids in mixtures were recovered with equal efficiency. Protein recovery was in the same range as that of lipids. The final (after sucrose gradient) recovery and lipid:protein molar ratio were assessed for each experiment. The Triton X-114 content in proteoliposomes was less than 1 molecule of detergent per 8000 molecules of lipids.

PLAP Transbilayer Distribution. The distribution of the enzyme between the two leaflets of the membrane was calculated on the basis of PI-PLC release experiments. The proportion of PLAP released by PI-PLC (outside-oriented enzyme) was varied from a minimum of 48% in the case of a POPC/30% Chol liposomes to a maximum of 63% in the case of a POPC/10% GM1 liposomes. These values were confirmed by assaying enzymatic activity, before and after treatment with Triton X-100 (data not shown).

Control experiments carried out with the purified enzyme showed that the activity was not affected by the presence of the detergent.

The proportion of outside-oriented PLAP was taken into account in the calculation of enzyme specific activity.

Influence of Protein:Lipid Molar Ratio on PLAP Activity. Proteoliposomes of a given lipid composition were prepared at different protein:lipid molar ratios. For each preparation, the final molar ratio, the extent of aggregation [judged on the basis of cross-linking by bis(sulfosuccinimidyl)suberate (BS^3)], and the enzyme activity were assessed. For a given lipid composition, the enzyme aggregation varied together with the protein:lipid molar ratio (~1:1000 to 1:5000, final) but did not affect the enzyme activity that was always comparable (data not shown), at least within the ratios that were tested. An example of the cross-linking technique is shown in Figure 2 for POPC/10% Chol proteoliposomes.

Effect of Liposome Composition on PLAP Kinetics. To evaluate the effect of lipid environment, the enzyme kinetics was studied on proteoliposomes with different lipid compositions at a final protein:lipid molar ratio of ~1:3000, and the results are reported in Figure 3. The enzyme exhibited comparable values of K_m, in a manner independent of liposome composition. On the other hand, different V_{max} values were observed when the liposome composition was changed, with lower values displayed by all the mixtures

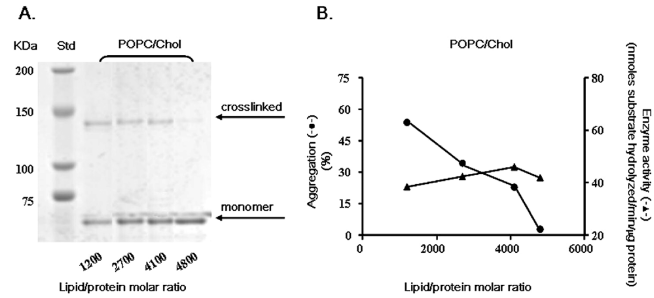

FIGURE 2: Activity and aggregation state of placental alkaline phosphatase, reconstituted in liposomes at different lipid:protein ratios. Illustration of the procedure utilized to assess the aggregation. Purified alkaline phosphatase was reconstituted at different protein:lipid molar ratios into liposomes composed of palmitoyloleoylglycero-3-phosphocholine (POPC) in a mixture with cholesterol (10% molar), and activity was assayed using the substrate *p*-nitrophenyl phosphate, as described in the text. (A) Liposomes were incubated with 0.5 mM bis(sulfosuccinimidyl)suberate (BS^3) for 45 min at 4 °C. After SDS−PAGE had been carried out, the gel was submitted to EZ-Blue staining. The arrows indicate the monomer (lower) and cross-linked form (upper). (B) Plot of enzyme activity (●) and protein aggregation (▲) of alkaline phosphatase at different protein:lipid ratios. Alkaline phosphatase was reconstituted at protein:lipid molar ratios of 1:1000, 1:3000, 1:4000, and 1:5000 (initial). The values reported are the final ratios after reconstitution. Protein aggregation is expressed as the ratio between the OD of digitized bands corresponding to the cross-linked and non-cross-linked protein in the SDS−PAGE gel of panel A.

containing cholesterol (Figure 3). In particular, the lowest (52 ± 3 nmol of *p*-nitrophenyl phosphate hydrolyzed per minute per microgram of protein) value was displayed by SCRLs. The comparison among binary mixtures of POPC mixed with SM or Chol with a molar concentration of up to 30% showed that the sterol exerts an inhibitory effect, while the sphingolipid scarcely influences enzyme activity (Figure 3C).

Liposome Size. The diameter of liposomes was measured by light scattering. Liposomes were discrete, almost monodisperse, populations of different sizes. Their values are listed in Table 1. The smallest liposomes were POPC/10% GM1 liposomes (59 ± 6 nm), while the largest were SCRL and POPC/30% Chol liposomes (185 ± 23 and 188 ± 25 nm, respectively). For each lipid mixture, the V_{max} value was plotted against the corresponding diameter (Figure 4): a strong relationship between the two variables was observed ($p < 0.0001$; correlation coefficient = 0.91).

In addition, the enzyme activity was evaluated on proteoliposomes having an identical composition (POPC) but a different size, obtained by insertion of the enzyme into vesicles obtained by extrusion through filters with pores with different diameters (100, 200, or 400 nm). The results (inset of Figure 4) show that the activity decreases with an increase in the proteoliposome diameter.

DPH Fluorescence Anisotropy. The values of DPH fluorescence polarization are reported in Figure 5 and show a maximum in the case of the SCRL. The plot of enzyme activity versus polarization shows a strong correlation. The data can be divided into two groups: one gathering samples with higher polarization and lower activity and sharing a common presence of cholesterol and a second group gathering samples displaying lower polarization and higher activity and sharing a common absence of cholesterol.

A weak correlation was observed between liposome diameter and DPH fluorescence polarization (data not shown).

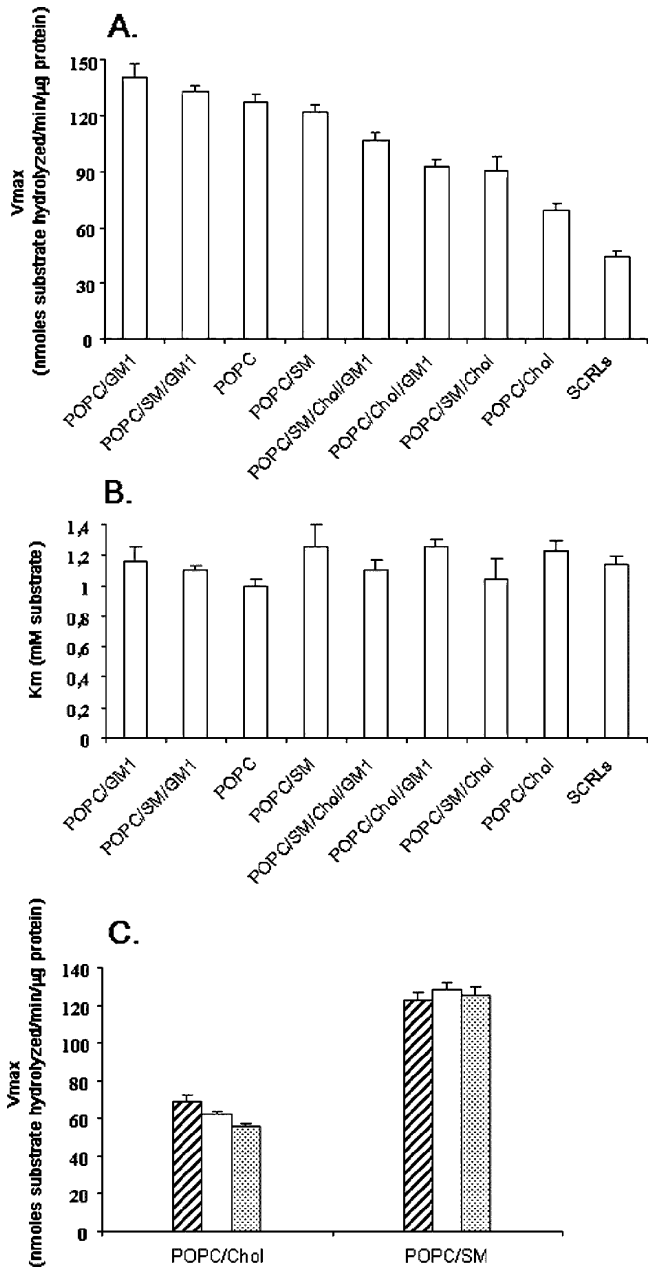

FIGURE 3: Kinetics of placental alkaline phosphatase reconstituted in liposomes. Purified alkaline phosphatase was reconstituted in proteoliposomes composed of palmitoyloleoylglycero-3-phosphocholine (POPC), alone or in a mixture with other lipids. The activity was assayed using *p*-nitrophenyl phosphate, at different concentrations, as the substrate (see the text for details). (A) V_{max} values calculated from the double-reciprocal $1/V$ vs $1/[S]$ plot, according to the Lineweaver−Burk method on proteoliposomes. Each of the lipids added to POPC represented 10% of the total molar mixture, with the exception of SCRLs that were composed of POPC, 34% Chol, 16% SM, and 16% GM1. Error bars are the standard deviation ($n = 5$). The correlation constants (c) were between 0.999 and 0.994. Differences in V_{max} between samples are statistically significant ($p < 0.05$) with the exception of POPC, which was not statistically different from POPC/10% SM/10% GM1 and POPC/10% SM liposomes; and POPC/10% Chol/10% GM1 liposomes, which were not statistically different from POPC/10% SM/10% Chol and POPC/10% SM/10% Chol/10% GM1 liposomes. (B) K_m values calculated from the double-reciprocal $1/V$ vs $1/[S]$ plot, according to Lineweaver−Burk analysis. Error bars are the standard deviation ($n = 5$). Differences in K_m between any couple of samples are not statistically significant. (C) V_{max} values calculated from the double-reciprocal $1/V$ vs $1/[S]$ plot, according to Lineweaver−Burk analysis, on binary proteoliposomes composed of POPC and different molar proportions (striped bar, 10%; white bar, 20%; dotted bar, 30%) of SM or Chol.

Table 1: Diameter (nanometers) of Liposomes Used in This Investigation, As Assessed by a Laser Light Scattering Technique

sample acronym in the text	diameter ± standard deviation (nm)
POPC	69 ± 7
POPC/10% SM	100 ± 10
POPC/30% SM	91 ± 9
POPC/10% Chol	148 ± 15
POPC/30% Chol	188 ± 25
POPC/10% GM1	59 ± 6
POPC/10% SM/10% Chol	137 ± 14
POPC/10% Chol/10% GM1	86 ± 9
POPC/10% SM/10% GM1	64 ± 6
POPC/10% SM/10% Chol/10% GM1	73 ± 7
POPC/16% SM/16% GM1/34% Chol (SCRL)	185 ± 23

DISCUSSION

GPI-anchored proteins are commonly found enriched within detergent-resistant membranes (DRMs), isolated from cells, and considered the experimental evidence of the existence of membrane lipid rafts (*4–8, 25–27*). Among the possible functional consequences, it has been suggested that apical sorting and transmembrane signaling occur by interaction of the GPI anchor with rafts (*8, 9*). Furthermore, in the context of their membrane trafficking pathways, GPI-anchored proteins are found to be retained in the recycling endocytic compartments longer than in other membrane compartments, and this behavior has been shown to depend on cellular levels of sphingolipid and cholesterol (*28, 29*).

Scant information is available concerning the influence of lipids on the activity of GPI-anchored, and generally of raft-associated, enzymes. Since several studies have demonstrated that model membranes provide a valuable tool for elucidating some of the raft properties (*19, 30–32*), in this investigation

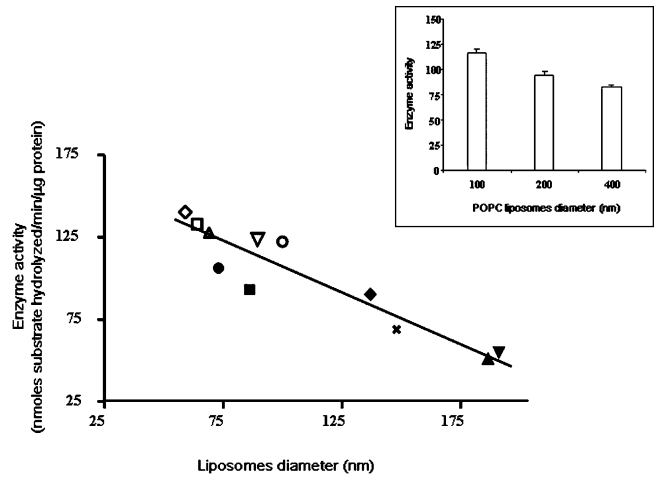

FIGURE 4: Relationship between activity of human placental alkaline phosphatase reconstituted in liposomes and liposome size. Enzyme activity of proteoliposomes composed of POPC (△) or POPC in a mixture with 10% SM (○), 10% GM1 (◇), 10% Chol (×), 10% SM and 10% GM1 (□), 30% SM (▽), 30% Chol (▼), 10% SM and 10% Chol (◆), 10% Chol and 10% GM1 (■), 10% SM, 10% Chol, and 10% GM1 (●), or 34% Chol, 16% SM, and 16% GM1 (SCRL, ▲) was plotted against the corresponding liposome size and submitted to statistical analysis (see the text for details). A significant relationship between the two variables was observed ($p < 0.0001$; correlation coefficient = 0.91). The inset shows the enzyme activity of proteoliposomes of different sizes and composed of POPC, obtained by the extrusion technique through filters with pores 100, 200, or 400 nm in diameter (see the text for details).

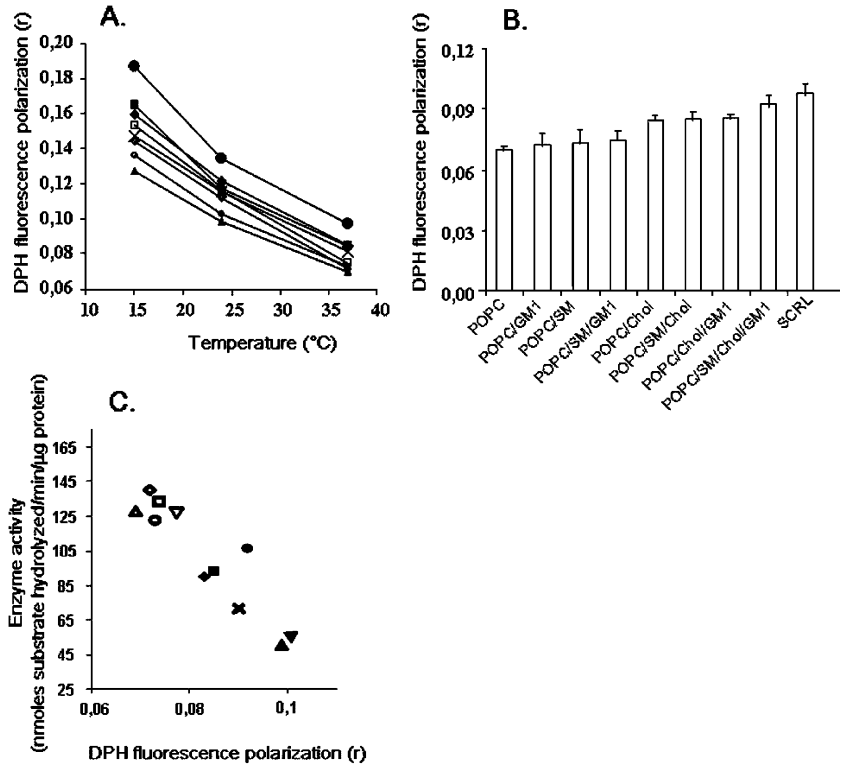

FIGURE 5: Fluorescence anisotropy of diphenylhexatriene in liposomes with different compositions. (A) Fluorescence polarization at different temperatures of the fluorescent probe diphenylhexatriene (DPH) in liposomes composed of POPC alone or in a mixture with other lipids. Values shown are from one representative experiment. (B) Fluorescence polarization of the fluorescent probe diphenylhexatriene in liposomes with different lipid compositions at 37 °C. Each of the lipids added to POPC represented 10% of the total molar mixture, with the exception of SCRLs that were composed of POPC, 34% Chol, 16% SM, and 16% GM1. (C) Relationship between the activity of placental alkaline phosphatase reconstituted in proteoliposomes and fluorescence polarization of diphenylhexatriene. Purified alkaline phosphatase was reconstituted into liposomes composed of POPC alone or mixed with other lipids. For each lipid composition, the value of V_{max} was plotted against the corresponding fluorescence polarization of diphenylhexatriene embedded in vesicles and submitted to statistical analysis (see the text for details). A significant relationship between the two variables was observed ($p < 0.05$; correlation coefficient = 0.78). Error bars are the standard deviation ($n = 4$). POPC (△) and POPC in a mixture with 10% SM (○), 10% GM1 (◇), 10% Chol (×), 10% SM and 10% GM1 (□), 30% SM (▽), 30% Chol (▼), 10% SM and 10% Chol (◆), 10% Chol and 10% GM1 (■), 10% SM, 10% Chol, and 10% GM1 (●), or 34% Chol, 16% SM, and 16% GM1 (SCRL, ▲).

we utilize a model membrane system based on proteoliposomes, in which the GPI-anchored protein human placental alkaline phosphatase (PLAP) has been functionally reconstituted and its kinetic properties have been correlated with the physicochemical features of the membrane.

POPC was chosen as the constituent of the bulk lipid matrix, because it is abundant in eukaryotic cells (*33*) and it is homogeneously distributed among cellular membranes (*34, 35*). Binary, ternary, and quaternary mixtures of POPC with sphingomyelin, ganglioside GM1, and cholesterol, i.e., lipids typically enriched within DRMs, were tested. Moreover, sphingolipid−cholesterol-rich liposomes (SCRL) were utilized as a lipid raft-mimicking system, according to previous suggestions (*15, 16*).

The kinetic studies carried out on proteoliposomes show that V_{max} is influenced by the presence of raft lipids in the POPC matrix and displays its lowest value when the enzyme is reconstituted in SCRL. The evaluation of POPC/sphingolipid and POPC/cholesterol binary mixtures suggests that the sterol may be responsible for the inhibition, while sphingolipids do not significantly affect the enzyme activity. As a further confirmation of the inhibitory effect of the sterol, it is worth noting that the activity of proteoliposomes containing cholesterol (binary, ternary, and quaternary) is lower than those without sterol.

Successively, the possibility that the aggregation state of the protein may affect its activity (*36*) was ruled out by the observation that proteoliposomes having the same lipid composition, but different PLAP:lipid molar ratios and different extents of aggregation of the protein, display comparable enzyme activity.

Then, we took into account the possibility that the curvature of the membrane may affect its activity: a strong significant inverse correlation with liposome size suggests that enzyme activity is negatively affected by larger curvature radii of the bilayer. However, since the observed changes in vesicle size follow changes in the cholesterol content of the membrane, it is not possible to establish if curvature is the more important physical property underlying the results. A response to this ambiguity was suggested by the comparison among proteoliposomes having different diameters but identical lipid compositions, the activity of which decreases with bilayers with larger curvature radii.

It is worth stressing that the effect of membrane curvature on the activity of GPI-anchored enzymes is here reported for the first time, even though it is known that this feature influences the activity of enzymes affecting the lipid bilayer or temporarily adhering to the membrane, such as protein kinase C (PKC) and phosphocholine cytidyl-transferase (CTP), as well as integral membrane protein segregation (*37–41*).

Finally, we took into account the possibility that the packing of the lipid bilayer where the enzyme is embedded may affect its activity. For this purpose, we performed experiments with steady-state fluorescence polarization, which is correlated to the rotational diffusion rate of the membrane-embedded probe, DPH; the samples containing cholesterol, displaying a more ordered (rigid) environment of the probe, also displayed lower activities.

Taken together, these results suggest that cholesterol-rich bilayers exert a negative control on enzyme activity. Since either cholesterol or GPI-anchored proteins are concentrated within lipid rafts, the results suggest that these membrane compartments may play an important role in the activity of PLAP.

This hypothesis is reinforced by previous results (*36, 42, 43*) obtained with other DRM-associated enzymes, among which is the virulence determinant GPI-anchored phospholipase B1 of the fungal pathogen *Cryptococcus neoformans*, the activity of which was inhibited in the raft environment.

One could question how differences in lipid environment, bilayer order, or curvature may affect the activity of a GPI-anchored enzyme. With regard to the first point, it has been suggested (*19, 27*) that the lipid environment could place conformational constraints on the GPI anchor and this, in turn, on the PLAP active site. Alternatively, lipids within the raft environment could impose the inhibition; it has been shown previously that the protein component of PLAP lies close to or is in direct contact with the lipid bilayer (*44*), potentially allowing the membrane lipids to influence its activity. With regard to the second point, it has been shown that the catalytic properties of GPI-anchored enzymes are influenced by the phase state and fluidity of the bilayer (*45*). Finally, with regard to curvature, our speculation is that the mutual spacing among the protein moieties of the enzyme, anchored with the GPI moieties, is larger in liposomes with greater curvature, facilitating the turnover of substrate molecules at the catalytic site. Membrane curvatures comparable with those of the smaller liposomes herein utilized may be encountered at the "neck" of caveolae where GPI-anchored proteins may occasionally move (*46–48*).

However, it should be remarked that this study was carried out on an artificial model system. Therefore, this is to be taken as speculation that deserves further evaluation in a cellular system.

Finally, it should be mentioned that a number of results indicate that lipid rafts contain only a portion of GPI-anchored proteins with respect to the rest of the membrane bilayer (*15, 25*). Therefore, PLAP molecules inside or outside these membrane compartments may express different activity; moreover, the affinity of PLAP for rafts or raft models may change depending on changes in lipid−lipid and lipid−protein interaction (*15*). Finally, the composition of DRMs in which PLAP is enriched is not certain, and it could be localized within cholesterol-poor subsets of DRM as other GPI-anchored proteins (*44*).

The challenge is now to increase the complexity of this minimal model system and mimic more closely the cellular context.

REFERENCES

1. Ferguson, M. A. (1999) The structure, biosynthesis and functions of glycosylphosphatidylinositol anchors, and the contributions of trypanosome research. *J. Cell Sci. 112*, 2799–2909.
2. Hooper, N. M. (1992) More than just a membrane anchor. *Curr. Biol. 2*, 617–619.
3. Nosjean, O., Briolay, A., and Roux, B. (1997) Mammalian GPI proteins: Sorting, membrane residence and functions. *Biochim. Biophys. Acta 1331*, 153–186.
4. Cinek, T., and Horejsi, V. (1992) The nature of large noncovalent complexes containing glycosyl-phosphatidylinositol-anchored membrane glycoproteins and protein tyrosine kinases. *J. Immunol. 149*, 2262–2270.
5. Harder, T., and Simons, K. (1997) Caveolae, DIGs, and the dynamics of sphingolipid-cholesterol microdomains. *Curr. Opin. Cell Biol. 9*, 534–542.
6. Hooper, N. M. (1999) Detergent-insoluble glycosphingolipid/cholesterol-rich membrane domains, lipid rafts and caveolae. *Mol. Membr. Biol. 16*, 145–156.
7. Rietveld, A., and Simons, K. (1998) The differential miscibility of lipids as the basis for the formation of functional membrane rafts. *Biochim. Biophys. Acta 1376*, 467–479.
8. Simons, K., and Ikonen, E. (1997) Functional rafts in cell membranes. *Nature 387*, 569–572.
9. Brown, D. A., and London, E. (2000) Structure and function of sphingolipid- and cholesterol-rich membrane rafts. *J. Biol. Chem. 275*, 17221–17224.
10. Schroeder, R., London, E., and Brown, D. A. (1994) Interactions between saturated acyl chains confer detergent resistance on lipids and glycosylphosphatidylinositol (GPI)-anchored proteins: GPI-anchored proteins in liposomes and cells show similar behaviour. *Proc. Natl. Acad. Sci. U.S.A. 91*, 12130–12134.
11. Laemmli, U. K. (1970) Cleavage of structural proteins during the assembly of the head of bacteriophage T4. *Nature 227*, 680–685.
12. Cyboron, G. W., and Wuthier, R. E. (1981) Purification and initial characterization of intrinsic membrane-bound alkaline phosphatase from chicken epiphyseal cartilage. *J. Biol. Chem. 256*, 7262–7268.
13. Lineweaver, H., and Burk, D. (1934) The determination of enzyme dissociation constants. *J. Am. Chem. Soc. 56*, 658–666.
14. Angrand, M., Briolay, A., Ronzon, F., and Roux, B. (1997) Detergent-mediated reconstitution of a glycosyl-phosphatidylinositol-protein into liposomes. *Eur. J. Biochem. 250*, 168–176.
15. Baron, G. S., and Caughey, B. (2003) Effect of glycosylphosphatidylinositol anchor-dependent and -independent prion protein association with model raft membranes on conversion to the protease-resistant isoform. *J. Biol. Chem. 278*, 14883–14892.
16. Schroeder, R. J., Ahmed, S. N., Zhu, Y., London, E., and Brown, D. A. (1998) Cholesterol and sphingolipid enhance the Triton X-100 insolubility of glycosylphosphatidylinositol-anchored proteins by promoting the formation of detergent-insoluble ordered membrane domains. *J. Biol. Chem. 273*, 1150–1157.
17. Mayer, L. D., Hope, M. J., Cullis, P. R., and Janoff, A. S. (1985) Solute distributions and trapping efficiencies observed in freeze-thawed multilamellar vesicles. *Biochim. Biophys. Acta 817*, 193–196.
18. Ronzon, F., Morandat, S., Roux, B., and Bortolato, M. (2004) Insertion of a glycosylphosphatidylinositol-anchored enzyme into liposome. *J. Membr. Biol. 197*, 169–177.
19. Kahya, N., Brown, D. A., and Schwille, P. (2005) Raft partitioning and dynamic behavior of human placental alkaline phosphatase in giant unilamellar vesicles. *Biochemistry 44*, 7479–7489.
20. Bartlett, G. R. (1959) Phosphorus assay in column chromatography. *J. Biol. Chem. 234*, 466–468.
21. Svennerholm, L. (1957) Quantitative estimation of sialic acids. II. A colorimetric resorcinol-hydrochloric acid method. *Biochim. Biophys. Acta 24*, 604–611.
22. Palestini, P., Pitto, M., Tedeschi, G., Ferraretto, A., Parenti, M., Brunner, J., and Masserini, M. (2000) Tubulin anchoring to glycolipid-enriched, detergent-resistant domains of the neuronal plasma membrane. *J. Biol. Chem. 275*, 9978–9985.
23. Giglioni, A., Pitto, M., Chigorno, V., Zorzino, L., and Ghidoni, R. (1990) Subcellular metabolism of exogenous GM1 ganglioside in normal human fibroblast. *Biochem. Int. 22*, 85–94.
24. Friedrichson, T., and Kurzchalia, T. V. (1998) Microdomains of GPI-anchored proteins in living cells revealed by crosslinking. *Nature 394*, 802–805.
25. Roper, K., Corbeil, D., and Huttner, W. B. (2000) Retention of prominin in microvilli reveals distinct cholesterol-based lipid microdomains in the apical plasma membrane. *Nat. Cell Biol. 2*, 582–592.
26. Brown, D. A., and Rose, J. K. (1992) Sorting of GPI-anchored proteins to glycolipid-enriched membrane subdomains during transport to the apical cell surface. *Cell 68*, 533–544.

27. Mayor, S., and Maxfield, F. R. (1995) Insolubility and redistribution of GPI-anchored proteins at the cell surface after detergent treatment. *Mol. Biol. Cell 6*, 929–944.
28. Mayor, S., Sabharanjak, S., and Maxfield, F. R. (1998) Cholesterol-dependent retention of GPI-anchored proteins in endosomes. *EMBO J. 17*, 4626–4638.
29. Chatterjee, S., Smith, E. R., Hanada, K., Stevens, V. L., and Mayor, S. (2001) GPI anchoring leads to sphingolipid-dependent retention of endocytosed proteins in the recycling endosomal compartment. *EMBO J. 20*, 1583–1592.
30. Ferraretto, A., Palestini, P., Pitto, M., and Masserini, M. (1997) Lipid domains in the membrane: Thermotropic properties of sphingomyelin vesicles containing GM1 ganglioside and cholesterol. *Biochemistry 36*, 9232–9236.
31. Simons, K., and Vaz, L. C. (2004) Model systems, lipid rafts, and cell membranes. *Annu. Rev. Biophys. Biomol. Struct. 33*, 269–295.
32. Milhiet, P. E., Domec, C., Giocondi, M. C., VanMau, N., Helz, F., and Le Grimellec, C. (2001) Domain formation in models of the renal brush border membrane outer leaflet. *Biophys. J. 81*, 547–555.
33. Ekroos, K., Ejsing, C. S., Bahr, U., Karas, M., Simons, K., and Shevchenko, A. (2003) Charting molecular composition of phosphatidylcholines by fatty acid scanning and ion trap MS3 fragmentation. *J. Lipid Res. 44*, 2181–2192.
34. Colbeau, A., Nachbaur, J., and Vignais, P. M. (1971) Enzymic characterization and lipid composition of rat liver subcellular membranes. *Biochim. Biophys. Acta 249*, 462–492.
35. Schneiter, R., Brugger, B., Sandhoff, R., Zellnig, G., Leber, A., Lampl, M., Athenstaedt, K., Hrastnik, C., Eder, S., and Daum, G. (1999) Electrospray ionization tandem mass spectrometry (ESI-MS/MS) analysis of the lipid molecular species composition of yeast subcellular membranes reveals acyl chain-based sorting/remodeling of distinct molecular species en route to the plasma membrane. *J. Cell Biol. 146*, 741–754.
36. Hinkovska-Galcheva, V., Boxer, L. A., Kindzelskii, A., Hiraoka, M., Abe, A., Goparju, S., Spiegel, S., Petty, H. R., and Shayman, J. A. (2005) Ceramide 1-phosphate, a mediator of phagocytosis. *J. Biol. Chem. 280*, 26612–26621.
37. Reynwar, B. J., Illya, G., Harmandaris, V. A., Müller, M. M., Kremer, K., and Deserno, M. (2007) Aggregation and vesiculation of membrane proteins by curvature-mediated interactions. *Nature 447*, 461–464.
38. Foti, M., Porcheron, G., Fournier, M., Maeder, C., and Carpentier, J. (2007) The neck of caveolae is a distinct plasma membrane subdomain that concentrates insulin receptor in 3T3-L1 adipocytes. *Proc. Natl. Acad. Sci. U.S.A. 104*, 1242–1247.
39. Ahyayauch, H., Villar, A. V., Alonso, A., and Goni, F. M. (2005) Modulation of PI-specific phospholipase C by membrane curvature and molecular order. *Biochemistry 44*, 11592–11600.
40. Slater, S. J., Kelly, M. B., Taddeo, F. J., Ho, C., Rubin, E., and Stubbs, C. D. (1994) The modulation of protein kinase C activity by membrane lipid bilayer structure. *J. Biol. Chem. 269*, 4866–4871.
41. Cornell, R. B. (1991) Regulation of CTP:phosphocholine cytidylyltransferase by lipids. 2. Surface curvature, acyl chain length, and lipid-phase dependence for activation. *Biochemistry 30*, 5881–5888.
42. Diaz, O., Mebarek-Azzam, S., Benzaria, A., Dubois, M., Lagarde, M., Nemoz, G., and Prigent, A. F. (2005) Disruption of lipid rafts stimulates phospholipase D activity in human lymphocytes: Implication in the regulation of immune function. *J. Immunol. 175*, 8077–8086.
43. Siafakas, A. R., Wright, L. C., Sorrell, T. C., and Djordjevic, J. T. (2006) Lipid rafts in *Cryptococcus neoformans* concentrate the virulence determinants phospholipase B1 and Cu/Zn superoxide dismutase. *Eukaryotic Cell 5*, 488–498.
44. Lehto, M. T., and Sharom, F. J. (2002) Proximity of the protein moiety of a GPI-anchored protein to the membrane surface: A FRET study. *Biochemistry 41*, 8368–8376.
45. Sharom, F. J., Lorimer, I., and Lamb, M. P. (1985) Reconstitution of lymphocyte 5′-nucleotidase in lipid bilayers: Behaviour and interaction with concanavalin A. *Can. J. Biochem. Cell Biol. 63*, 1049–1057.
46. Wang, J., Gunning, W., Kelley, K. M., and Ratnam, M. (2002) Evidence for segregation of heterologous GPI-anchored proteins into separate lipid rafts within the plasma membrane. *J. Membr. Biol. 189*, 35–43.
47. Sens, P., and Turner, M. S. (2006) The forces that shape caveolae, in *Lipid Rafts and Caveolae* (Fielding, C. J., Ed.) pp 25–34, Wiley-VCH Verlag GmbH & Co. KGaA, Weinhein, Germany.
48. Oh, P., McIntosh, D. P., and Schnitzer, J. E. (1998) Dynamin at the neck of caveolae mediates their budding to form transport vesicles by GTP-driven fission from the plasma membrane of endothelium. *J. Cell Biol. 141*, 101–114.

BI800005S